

Changing the Beutler-Fano Profile of the Ne(ns') Autoionizing Resonances

J. Ganz, M. Raab, H. Hotop, and J. Geiger

Fachbereich Physik der Universität, D-6750 Kaiserslautern, Federal Republic of Germany

(Received 16 July 1984)

We show both experimentally and by a semiempirical multichannel quantum-defect-theory analysis that the profile of the Ne($ns', J=1$) autoionizing resonances varies with the character of the Ne($2p^5 3p, J=1, 2$) state, from which the resonance is excited, whereas the resonance width is constant.

PACS numbers: 32.80.Dz, 32.80.Fb

In a two-step laser excitation experiment¹ involving a metastable Ne($3s^3P_{2,0}$) beam, we have recently studied the lowest Ne(ns', nd') autoionizing resonances with a resolution (4 GHz) which allowed for the first time a reliable determination of the width Γ of the Ne($14s', J=1$)— $\Gamma=6.0(5)$ GHz—and of the Ne($12d', J=2, 3$)— $\Gamma=2.0(5)$ GHz—resonances. In this way, the relativistic multichannel quantum-defect theory (RMQDT) prediction of Johnson and LeDourneuf² was confirmed that for Ne—in contrast to Ar, Kr, and Xe—the $ns'(J=1)$ resonances are distinctly broader than the $nd'(J=1)$ resonances. Quantitatively, the experimental numbers¹ were about a factor of 2 below the *ab initio* theoretical values,² but agreed very well with more recent semiempirical nonrelativistic (MQDT) predictions.¹ A more detailed study with even better resolution, with use of a single-mode dye laser, is highly desirable in order to accurately determine the width Γ and the profile index q for the various Ne(ns', nd') resonances. We have now carried out such experiments and, stimulated by MQDT predictions outlined below, investigated the dependence of q for the Ne($ns', J=1$) resonances on the chosen intermediate state, as will be discussed in this Letter. The results for the other resonances Ne($ns', J=0$) and Ne($nd', J=1, 2, 3$) will be presented elsewhere.

MQDT describes the spectroscopic behavior of an atom or a molecule by only a few parameters, the eigen quantum defects μ_α , the dipole transition amplitudes D_α , and an orthogonal transformation matrix $U_{i\alpha}$, which connects the close-coupled channels α with the jj -coupled dissociation channels i . MQDT interlinks the conventional spectroscopic description with the collision theory. This allows the application of well-developed and illustrative concepts from the field of atomic collisions. Thus there may be cases which are rather difficult to understand from a spectroscopic point of view, whereas the collisional approach gives an easy insight into the essential process. The present study is an example for the latter case.

Though it is known³ that the interaction between

the $J=1$, s and d series in neon is nonzero, an MQDT analysis of the two s channels alone is a fairly good approximation.⁴ The continuum oscillator strength of a two-channel resonance can be written as⁵

$$\frac{1}{E} \frac{df(\nu)}{dE} = I_0 \sin^2 \pi(\tau - \tau_z). \quad (1)$$

Equation (1) has the same form as the cross section for electron scattering near a resonance. The phase shift $\pi\tau$ is extracted from a Lu-Fano plot⁶ $\tau = f(\nu)$, which can be constructed from the atomic energy levels. ν is the effective quantum number, related to the upper ionization limit, and τ is the quantum defect, modulo 1, related to the lower ionization limit. Figure 1 is an illustrative model. The rapidly varying part of the Lu-Fano plot [Fig. 1(c)] gives rise to the resonance. The slope of the phase $\pi\tau$ at the position of the resonance fixes the width Γ of the resonance profile.

The value τ_z in Eq. (1) determines that quantum defect τ where the oscillator strength is zero. It is closely connected to the profile index q . This can be seen from the following consideration. The probability amplitude $J(\nu)$ for radiating transitions can be represented⁵ by

$$J(\nu) = [D_\alpha A_\alpha(\nu)]. \quad (2)$$

The mixing coefficients A_α which set the contribution of the close-coupling states $\alpha=1, 2$ involve simply a trigonometric function:

$$A_1 = a_1 \sin \pi(\mu_2 - \tau), \quad A_2 = a_2 \sin \pi(\mu_1 - \tau), \quad (3)$$

where τ depends on the effective quantum number ν and a_1 and a_2 are constants. In order to find the two-channel close-coupling eigenstates, one takes advantage of the Lu-Fano plot [Fig. 1(c)]: The intersections of the diagonal $\tau = 1 - \nu$ with the curve $\tau = f(\nu)$ determine the positions of the states α and hence the eigen quantum defects μ_α . According to Eqs. (2) and (3) at $\tau = \mu_2$ only D_1 and at $\tau = \mu_1$ only D_2 contribute to the oscillator strength. Since for the $J=1$ states of neon the matrix $U_{i\alpha}$ is very nearly an LS - jj transformation matrix, the close-coupling states should be LS states (Lu⁷). In this

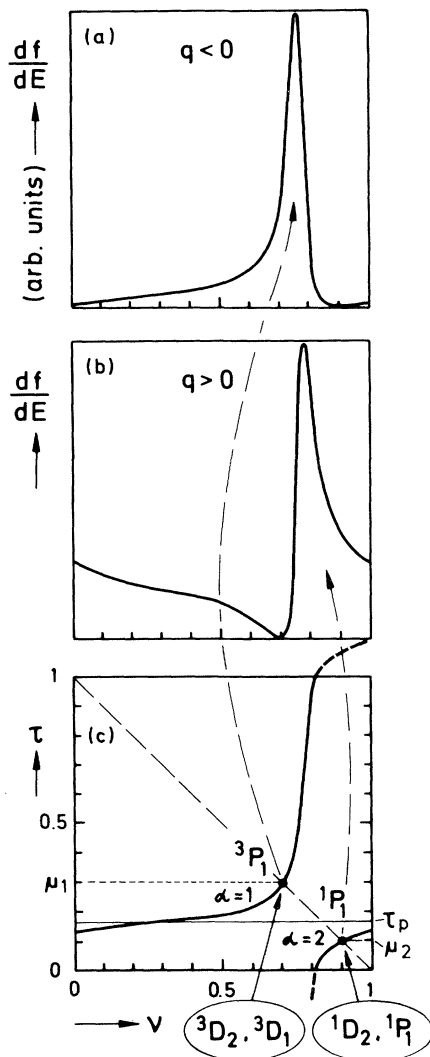


FIG. 1. Resonance profiles showing the change of the shape of the resonance if either (a) the close-coupling state $\alpha=1$ or (b) the state $\alpha=2$ is excited; (c) the Lu-Fano plot. The diagrams are purely schematic; model parameters where $\mu_1=0.3$, $\mu_2=0.1$, $\beta=0.615$. τ and ν are plotted modulo 1. A neon Lu-Fano plot can be found in Ref. 4.

case the state $\alpha=1$ has triplet and the state $\alpha=2$ has singlet character. This has the following consequences: If the autoionizing state is excited from a singlet state, then, because intercombination is forbidden, the state $\alpha=2$ is excited only. Following Eqs. (2) and (3) we expect an autoionizing profile with zero oscillator strength at $\tau_z = \mu_1$ or $\nu = 1 - \mu_1$ and a broad wing extending to the right and, because of the periodicity, continuing from the left in Fig. 1(b). If the lower level is a triplet state, then the state $\alpha=1$ is excited. Zero oscillator strength is now expected at $\tau_z = \mu_2$ or $\nu = 1 - \mu_2$ and the

broad wing to extend to the left in Fig. 1(a). If the originating level has a mixed singlet-triplet character, the autoionizing profile should deviate in a characteristic way from these special cases, and τ_z has to be determined from the ratio D_1/D_2 according to Eq. (44) of Ref. 5.

In the case of a sharp resonance the profile index q can be written as⁵

$$q = -\cot\pi(\tau_p - \tau_z). \quad (4)$$

The "plateau value" τ_p is given by

$$\tan \frac{1}{2}\pi(\mu_2 - \mu_1)\cos 2\beta = \tan \pi[\tau_p - (\mu_1 + \mu_2)/2],$$

where β is the angle generating the matrix $U_{i\alpha}$. Using the parameters based on a careful fitting procedure,⁸ $\mu_1=0.31445$, $\mu_2=0.2829$, $\beta=0.606$ rad, and $\tau_p=0.2931$, one finds from Eq. (4) for the profile indices of the two special cases discussed above, $q = +14.9$ and $q = -31.1$, respectively.

Now we briefly describe our experiment. A well-collimated (1:400), thermal velocity (800 m/s), metastable $\text{Ne}(3s^3P_{2,0})$ beam from a differentially pumped discharge source is transversely excited by two linearly polarized single-mode dye lasers. Photoions are detected with a quadrupole mass spectrometer with an electron multiplier and fast electronics. A stabilized red-yellow single-mode dye laser (DCM, Rh6G) excites either the $^{20}\text{Ne}(3s^3P_0)$ or the $^{20}\text{Ne}(3s^3P_2)$ fraction of the atomic beam (densities around $10^6/\text{cm}^3$) to the intermediate $\text{Ne}(3p, J=1, 2)$ state of interest (see Table I); a tunable blue single-mode dye laser (Stilben 3 or 1) excites the intermediate state to the continuum. The energy dependence of the photoionization cross section of the chosen $\text{Ne}(3p, J=1, 2)$ intermediate state has been measured by simultaneous multichannel scaling of the photoion count rate, the total intensity of the ionizing laser, and the transmission fringes of a calibrated confocal Fabry-Perot interferometer [free spectral range 150.0(2) MHz]. The overall resolution of this experiment was < 50 MHz, with a negligible contribution from Doppler broadening (< 10 MHz). The intensity of the red-yellow laser was attenuated to levels such that the dynamic Stark effect was negligible. The intensity of the ionizing laser (typically 30 mW on 1 mm^2) was too low to cause significant saturation effects. For the $\text{Ne}(14s', J=1)$ resonance, typical peak counting rates were 500 s^{-1} .

Figure 2 shows the results for the $\text{Ne}(14s', J=1)$ resonance, excited from four different $\text{Ne}(3p)$ intermediate states, which, from top to bottom, attain more and more triplet character (see, for example, Schectman⁹). One recognizes a clear change in the

TABLE I. Measured and calculated profile index q and width Γ of the $\text{Ne}(14s', J=1)$ autoionizing resonance. The ratios of the oscillator strengths (Ref. 10) for transitions between the intermediate $2p_n$ state and the states $1s_2$ and $1s_4$, respectively, are also given. The rows are arranged according to decreasing profile index q as measured.

| Intermediate $\text{Ne}(2p_n)$ states (Paschen notation) | Expt. Γ (GHz) | q | MQDT | | $\Delta\nu, \Gamma$ (GHz) | $\frac{f(1s_2^1P_1)}{f(1s_4^3P_1)}$ |
|--|----------------------------|-------------|------------------|--------------------|--|-------------------------------------|
| | | | q , pure LS | q , f ratio | | |
| $2p_5^1P_1$ | 5.54 ± 0.15 | $+29 \pm 3$ | +14.9 | +35 | $\Delta\nu = 5.47$ (five channels), ^a | 39.2 |
| $2p_6^1D_2$ | 5.31 ± 0.15 | $+10 \pm 1$ | | +11 | | 4.8 |
| $2p_7^3D_1$ | 5.49 ± 0.15 | -9 ± 1 | -31.1 | -13 | $\Gamma = 4.5$ (two channels) | 0.0693 |
| $2p_8^3D_2$ | 5.52 ± 0.15 | -13 ± 2 | | -6 | | 0.124 |

^aFrom Ref. 1.

resonance shape whereas—as expected—the resonance width Γ is constant [average value $\Gamma = 5.45(15)$ GHz]. The resonance parameters Γ and q , given in Table I, have been obtained from least-squares fits to the data points (represented by the smooth lines in the figures), with use of the following description of the cross section $\sigma(E)$ as a function of photon energy E around the resonance energy E_0 :

$$\sigma(E) = \sigma_{nc} + \sigma_{rc} \frac{(q + \epsilon)^2}{(1 + \epsilon^2)}, \quad (5)$$

$$\epsilon = (E - E_0) / (\frac{1}{2}\Gamma).$$

Here, σ_{nc} contains the contributions from the noninterfering background continuum and the second term describes a Beutler-Fano profile for the interaction of the resonance with the relevant interfering continua. Studies of several $\text{Ne}(ns', J=1)$ resonances with n around 22 resulted in Γ values with the expected ν^{-3} scaling with numbers for q in agreement with the ones determined for $n=14$. Good agreement for these widths Γ is found with the MQDT¹ width at half maximum $\Delta\nu = 1.7 \times 10^{-3}$ (5.47 GHz for $14s', J=1$), if all five channels were included. In the two-channel approximation the width is a little smaller, $\Gamma = 4.5$ GHz.

The results for the profile index q need a more detailed discussion. Table I shows that the experimental values q agree in the sign, but concerning the magnitude, only approximately with the two MQDT values calculated above, under the assumption that the transition amplitude goes either into the closing-coupling state $\alpha=1$ or $\alpha=2$. The reason is that the intermediate states are neither pure singlet nor pure triplet states. Therefore, as in the case of the transitions from the ground state where the resonance profile was determined by fitting to the oscillator strengths in the discrete,⁸ the same should be done for transitions from the intermediate states. An accurate and satisfactory fitting,

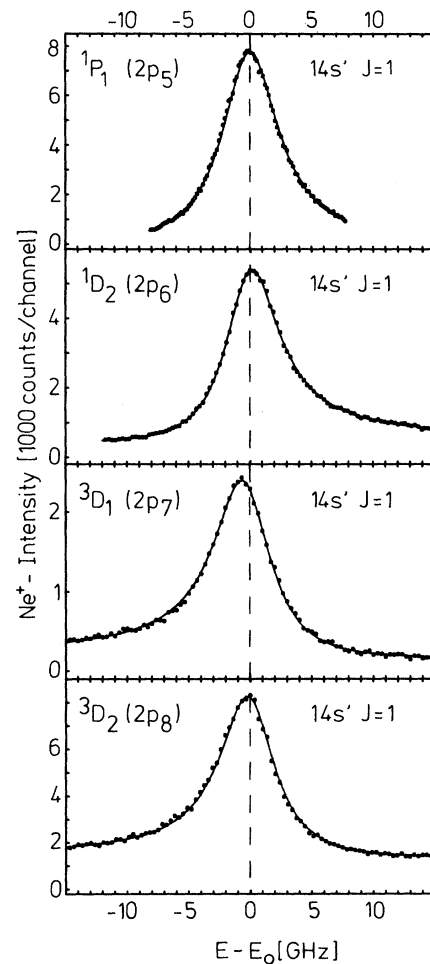


FIG. 2. Photoionization cross section of four different $\text{Ne}(2p^5 3p, J=1, 2)$ states in the region of the $\text{Ne}(14s', J=1)$ autoionizing resonance, measured with an overall resolution of ≤ 50 MHz. The smooth line through the data points is a least-squares fit using a Beutler-Fano profile, Eq. (5), with the parameters Γ and q given in Table I.

however, is prevented by the lack of available data for the oscillator strengths. Fortunately, at least the transition probabilities of the $2p$ - $1s$ transition (Paschen notation) are accurately known.¹⁰ Thus the relative contributions to the singlet and triplet close-coupling eigenstate can be estimated from the ratios of the corresponding oscillator strengths $f(1s_2)/f(1s_4)$. These ratios are given in the last column of Table I. They vary rather systematically with the exception of $2p_8$. The knowledge of this pair of oscillator strengths allows the transition matrix elements D_α to be determined empirically. By application of Eq. (44) of Ref. 5, τ_z , and use of Eq. (4), q were calculated. These values q are listed in Table I for comparison. They agree well with the measured values of the profile index q , again less so for the transition from the intermediate state $2p_8$. The reason for this might be that in this transition the contribution of singlet-triplet mixing and of s_2 - s_4 configuration interaction to the transition probability is strongest and hence is most sensitive to any numerical inaccuracy during the fitting procedure. Also the s - d interaction may play a role.

This work was supported in part by the Deutsche

Forschungsgemeinschaft (SFB 91) and by the Bundesministerium für Forschung und Technologie. We thank H. Rinneberg and E. Matthias for discussions and the loan of the Fabry-Perot marker cavity. We gratefully acknowledge the collaboration with K. Harth and M.-W. Ruf.

¹J. Ganz, A. Siegel, W. Bussert, K. Harth, M.-W. Ruf, H. Hotop, J. Geiger, and M. Fink, *J. Phys. B* **16**, L569 (1983).

²W. R. Johnson and M. LeDourneuf, *J. Phys. B.* **13**, L13 (1980).

³B. Edlén, *Handbuch der Physik*, edited by S. Flügge (Springer, Berlin, 1964), Vol. 27, p. 80.

⁴A. F. Starace, *J. Phys. B* **6**, 76 (1973).

⁵U. Fano, *Phys. Rev. A* **2**, 353 (1970), and *Phys. Rev. A* **15**, 817(E) (1977).

⁶K. T. Lu and U. Fano, *Phys. Rev. A* **2**, 81 (1970).

⁷K. T. Lu, *Phys. Rev. A* **4**, 579 (1971).

⁸J. Geiger and M. Fink, to be published.

⁹R. M. Schectman, D. R. Shoffstall, D. G. Ellis, and D. A. Chojnacki, *J. Opt. Soc. Am.* **63**, 80 (1973).

¹⁰P. Hartmetz and H. Schmoranzler, *Phys. Lett.* **93A**, 405 (1983).